Pergamon

0301-9322(94)00086-7

Int. J. Multiphase Flow Vol. 21, No. 4, pp. 591–606, 1995

0301-9322/95 $9.50 + 0.00

A SINGLE-STAGE HIGH PRESSURE STEAM INJECTOR FOR NEXT GENERATION REACTORS: TEST RESULTS AND ANALYSIS

G. CATTADORI[1], L. GALBIATI[2]†, L. MAZZOCCHI[2] and P. VANINI[3]

[1]SIET, Piacenza, Italy
[2]CISE Tecnologie Innovative, Segrate, Milan, Italy
[3]R & D Department, Nuclear Division, ENEL, Rome, Italy

(Received 24 October 1993; in revised form 25 October 1994)

Abstract—Steam injectors can be used in advanced light water reactors (ALWRs) for high pressure makeup water supply; this solution seems to be very attractive because of the "passive" features of steam injectors, that would take advantage of the available energy from primary steam without the introduction of any rotating machinery. The reference application considered in this work is a high pressure safety injection system for a BWR; a water flow rate of about 60 kg/s to be delivered against primary pressures covering a quite wide range up to 9 MPa is required. Nevertheless, steam driven water injectors with similar characteristics could be used to satisfy the high pressure core coolant makeup requirements of next generation PWRs. With regard to BWR application, an instrumented steam injector prototype with a flow rate scaling factor of about 1:6 has been built and tested. The tested steam injector operates at a constant inlet water pressure (about 0.2 MPa) and inlet water temperature ranging from 15 to 37°C, with steam pressure ranging from 2.5 to 8.7 MPa, always fulfilling the discharge pressure target (10% higher than steam pressure). To achieve these results an original double-overflow flow rate-control/startup system has been developed‡.

Key Words: steam injector, jet pumps, condensing injector, condensing injector

1. INTRODUCTION

A steam injector (SI) is a device without moving parts, in which steam is used as the energy source to pump cold water from a pressure lower than the steam to a pressure higher than the steam. In fact, a large amount of heat, available from steam condensation, can be partly converted into mechanical work useful for pumping the liquid. In this respect, the SI can be regarded as equivalent to different devices, like turbine-driven pumps, where steam thermal energy is used to pressurize a liquid; in comparison to this kind of equipment, the main difference is that in the SI all thermodynamic processes rely on direct contact transport phenomena (mass, momentum and heat transfer) between fluids, not requiring any moving mechanism. A simplified SI and pressure variation schematic is shown in figure 1. The SI can be divided into the following regions:

(a) the steam nozzle, producing a nearly isentropic expansion and partially converting steam enthalpy into kinetic energy; it can be a sonic nozzle or, if a stronger expansion is required, a supersonic nozzle with a typical converging–diverging shape;
(b) the water nozzle, producing a moderate acceleration and distributing the liquid all around the steam nozzle outlet;
(c) the mixing section, where steam and water come into contact. Steam transfers to water heat (because of temperature difference), mass (because of the related condensation) and momentum (because of velocity difference). The final result is the complete steam condensation, with an outflowing subcooled liquid at a relatively high pressure. The

†All correspondence should be addressed to: Dr L. Galbiati, Cise, Thermal and Fluid Dynamic Processes Section, C.P. 12081—20134 Milano, Italy.
‡Patent pending.

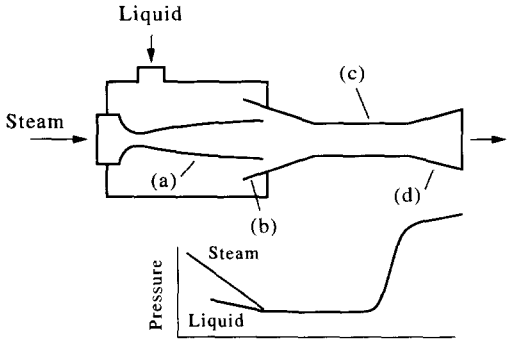

Figure 1. Schematic of the steam injector (SI): (a) steam nozzle; (b) water nozzle; (c) mixing section; and (d) diffuser.

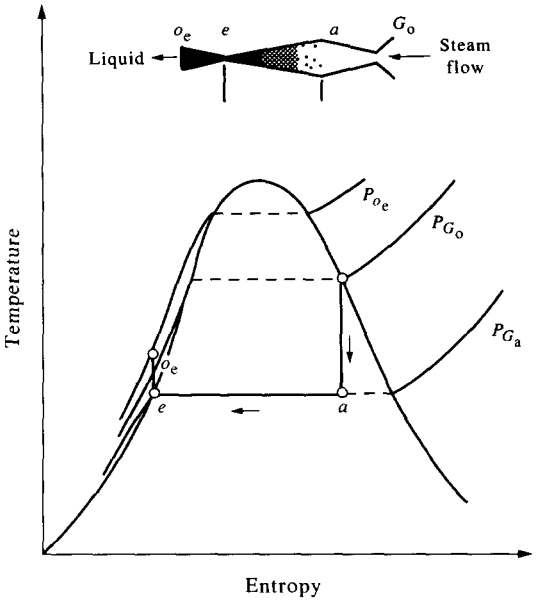

Figure 2. Mollier-diagram presentation of the ideal SI processes.

shape of the mixing section is usually converging, for reasons reported by Cattadori *et al.* (1992);

(d) the diffuser, where the liquid kinetic energy at the mixing section outlet is partially recovered producing a further pressure rise.

In figure 2 a Mollier-diagram presentation of the ideal SI processes is reported: the adiabatic steam expansion from P_{G_o} to P_{G_a} is shown as taking place through a converging–diverging nozzle, the condensation takes place in a convergent duct, the final adiabatic stagnation pressure P_{o_e} is achieved in an ideal liquid diffuser.

It should be noted that the arrangement of steam and water nozzles could be inverted, creating a circular water nozzle and an annular steam nozzle as reported by Fitzsimmons (1990). In another type of arrangement, reported by Narabayashi *et al.* (1992), the annular water jet is accelerated both by a central and outer steam jet. However, it is the authors' opinion that the central steam jet/outer liquid configuration should be more convenient because it minimizes the perimeter of the steam nozzle and avoids direct contact between the steam and mixing section walls; in this way viscous dissipations should be reduced.

SIs have been used as feedwater supply devices in locomotives and in the Merchant Marine since World War II and are manufactured by a few companies for applications in the food and paper industry. In the nuclear field, several systems based on high pressure steam injectors have been proposed: Howard (1984), Suurman (1986), Christensen *et al.* (1987), Narabayashi *et al.* (1991). With respect to this, the attractiveness of SIs is quite evident, because a high pressure water supply can be essential to very important emergency functions (like emergency core cooling, feedwater supply for decay heat removal and so on) and usually a steam supply is easily available in power plants. Moreover, SI can be regarded to a great extent as a passive system, as it does not require any external energy supply or moving mechanical part. However, commercially available SIs operate at "low" pressure (<2 MPa) and no single-stage high pressure steam injector is available from previous research programs undertaken by Suurman (1986), Fitzsimmons (1990) and Narabayshi *et al.* (1991).

In 1991, ENEL, the Italian Electricity Generating Board, which is engaged in a wide range of activities concerning ALWRs, decided to evaluate the applicability of a single-stage SI for a BWR; so CISE was instructed to perform a SI development study in co-operation with ENEL itself. The development process is described in Cattadori *et al.* (1992). In the same study, the maximum break

Table 1. Required water flow-rate Γ_1 vs reactor system pressure. Note that the indicated values refer to the net water flow set to the RCS and do not include the steam flow condensed in the SI

P_{G_0} (MPa)	Γ_L (kg/s)
8.7	58.0
8	55.3
6	45.0
4	33.2
2	19.4
1	12.0

size and the break location for SI design were specified. In summary, general requirements were assumed as follows:

(1) the SI must be able to supply the reactor system with a water flow rate corresponding to a 2 in. sch. 80 pipe break in the bottom region of the reactor vessel (continuous discharge of saturated liquid is assumed). The flow rate values, estimated by the homogeneous equilibrium model are shown in table 1;
(2) the SI must satisfy requirement (1) for a reactor system pressure ranging from 1 to 8.7 MPa;
(3) the required water pressure must be 10% more than the steam pressure (considering that it is sufficient to overcome the pressure drop along the steam and water piping).

2. EXPERIMENTAL SET-UP

According to the results obtained with a feasibility study, a preliminary SI sizing was possible and a scaled-down model (flow rate scale of about 1:6) operating at a prototypical temperature and pressure was designed by CISE. The model was made of stainless steel, its general initial arrangement being shown in figure 3. It should be noted that, as suggested by Fitzsimmons (1990), it was decided to perform the initial injector configuration development with a "smooth" mixing chamber, i.e. all sorts of openings in the converging section that are usually provided for the startup line were eliminated. Nevertheless (as shown in the following chapters) SI start-up was found to be impossible without overflow. In figure 4 the final test section configuration is shown. As can be seen, two overflow openings (primary and secondary overflows) were realized and the mixing chamber was directly connected to the diffuser. In fact, a constant area mixing section appeared to be unnecessary. The principal dimensions of the final test section are shown in table 2.

The SI was tested at SIET laboratories where a steam–water test facility was designed and built. Figure 5 shows a schematic diagram of the experimental plant which supplies metered flows of steam and water to the test section and which includes equipment for controlling and measuring the thermalhydraulic parameters. An open loop including pumps, heat exchangers and a pressurizer (volume = 1 m^3) provided demineralized water to the SI at the required conditions; water flow rates up to 25 kg/s were available, with fluid pressure and subcooling controlled at the test section inlet. A line coming from an external boiler provided superheated steam up to a 5 kg/s flow rate and 9 MPa pressure; liquid injection was used to control the steam temperature at the test section inlet. Open-system operation was straightforward, with the total discharge directed to the condenser. The test selection discharge pressure was varied by means of a control valve. The following measurements were taken during the tests:

- inlet liquid and steam flow rates;
- inlet and outlet fluid pressures and temperatures;

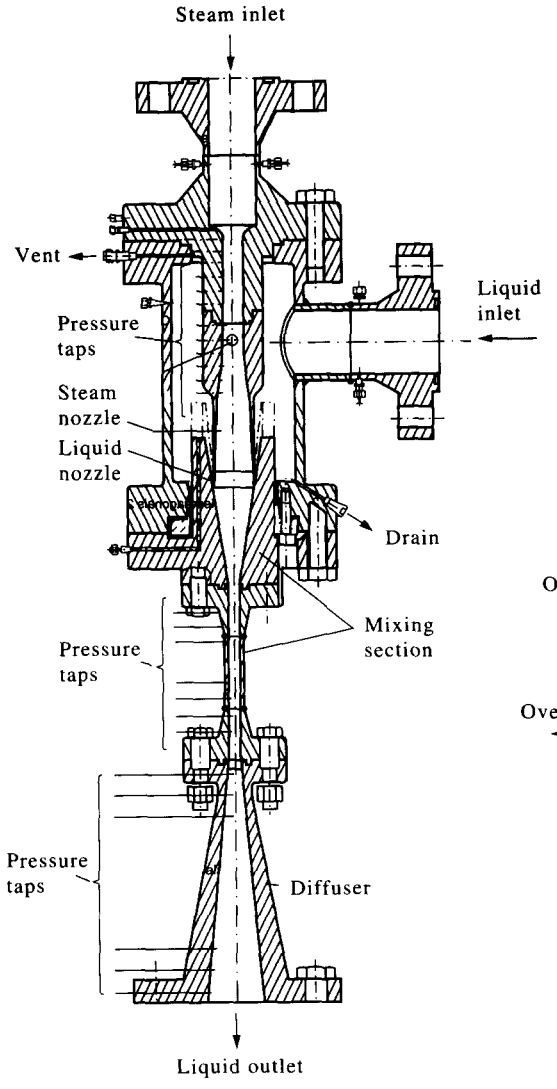

Figure 3. Test section with a "smooth" mixing section.

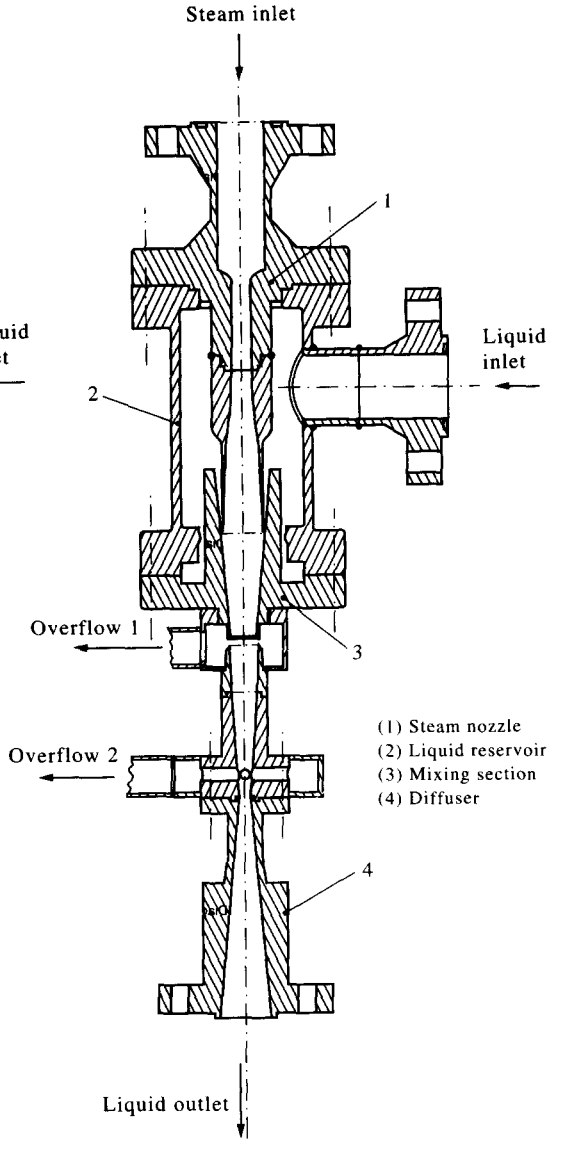

Figure 4. Test section: best configuration with primary and secondary overflow.

- axial pressure profiles in the different SI components: steam nozzle, water nozzle, mixing section, diffuser (in total 60 measurement stations);
- primary and secondary overflow temperatures and flow rates.

Flow rates were measured by means of calibrated orifice plates (accuracy = 2% of reading). Temperatures and pressures were measured by K-type thermocouples (accuracy = 1°C) and by thin film-type pressure transmitters (accuracy = 0.1% FS), respectively.

Table 2. Main design parameters of the test section

Steam nozzle throat diameter	22 mm
Steam nozzle outlet diameter	60 mm
Steam nozzle length	400 mm
Liquid nozzle width	5.2 mm
Mixing section contraction ratio (A_a/A_c)	20
Contraction ratio at the OF2 section (A_a/A_{OF2})	12
Mixing section convergence half angle	3°
Diffuser half angle	6°
Total length	1300 mm

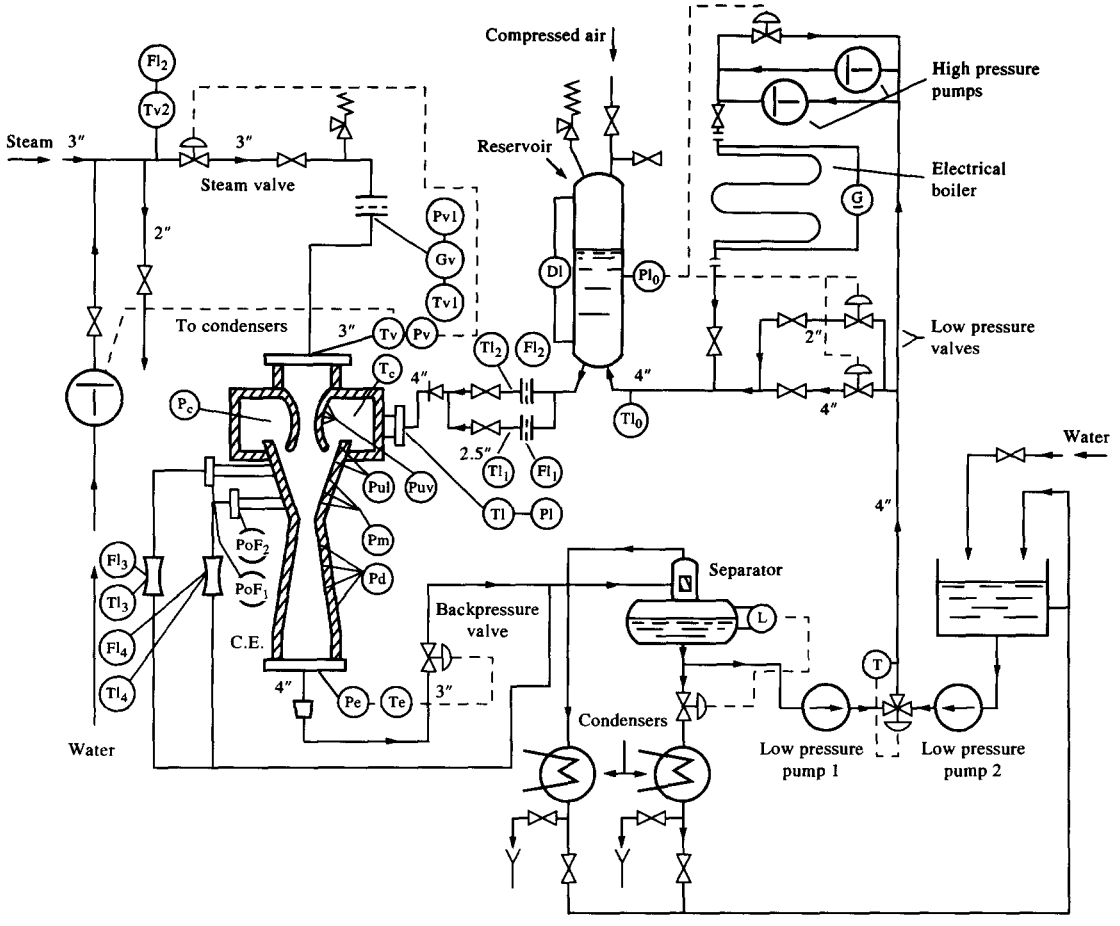

Figure 5. Schematic of the test facility.

3. TEST RESULTS AND DISCUSSION

Independent and dependent variables

There were four independent variables to be controlled or selected for each test run. These four can be described as:

- steam supply pressure;
- steam superheat;
- water supply pressure;
- water supply temperature.

To these four independent variables, concerning the fluid conditions, should be added:

- the backpressure valve setting;
- the OF2 valve setting (the OF1 valve could be always closed after startup).

On the other hand, several dependent variables (for any given set of independent variables) were selected and measured. These were:

- water supply flow rate;
- water–steam flow rate ratio (ω);
- steam nozzle pressures;
- mixing section pressures;
- primary and secondary overflow pressures/flow rates;

Table 3. Range of independent variables

Steam supply pressure	2.5–8.7 MPa
Steam superheat	5–30°C (max. steam quality = 1.1)
Water supply pressure	200–260 kPa
Supply water temperature	15–37°C

- diffuser pressures;
- discharge liquid pressure;
- discharge liquid temperature.

The range of the independent variables explored in the test program is shown in table 3. As can be noticed, the tests were conducted over a wide range of steam pressures (2.5–8.7 MPa). Steam superheat was also varied (between 3 and 30°C). In order to simulate real operating conditions, the water flow rate to the test selection was varied by adjusting the supply pressure between 200 and 260 kPa. The inlet water temperature was varied from 15 to 37°C. The reason for this was to check the injector's expected performance degradation at increased water temperature.

Most of the dependent variable variations will be discussed in the following paragraphs. However, the main dependent parameter variations are summarized in table 4. It can be seen that the inlet water flow rate range for the tests was about 14–21 kg/s and the liquid-to-steam flow rate ratio (ω) ranged between 3 and 14. ω is a significant variable because the principle of operation of the SI relies on the steam being condensed by the water in the mixing section and producing a vacuum. If the water–steam flow rate ratio is too low, the steam will not be completely condensed in the mixing section. On the other hand, according to the available theories, the maximum pressure which can be developed by the injector decreases as the water–steam ratio increases. thus for the best pressure performance, the injector should be operated at a low water–steam ratio but not so low that the steam will not condense completely. The water–steam flow ratio for a test could be varied by changing the steam supply pressure to the injector: the lower limit, for which condensation can be complete, depending also on the backpressure setting, was found to be about 3.

Steam nozzle performance

In order to calculate the steam flow rate, a homogeneous equilibrium model was used (expansion occurs in the wet region, so the hypothesis of a homogeneous steam–water flow has been assumed). Calculation results are shown in figure 6: calculated and measured values match each other very well. The steam expansion was very strong and sub-atmospheric values were reached at low and medium inlet steam pressures. In particular, using an experimental average expansion ratio, the steam nozzle outlet pressure (P_{G_a}) can be related to the inlet steam pressure (P_{G_o}) by the following expression:

$$P_{G_a} = \frac{P_{G_o}}{64} \qquad [1]$$

Using the measured steam nozzle outlet pressure and assuming an isentropic equilibrium flow, a theoretical steam nozzle exit area (A_{th}) can be calculated as:

$$A_{th} = \frac{\Gamma_G}{\rho_{G_a} u_{G_a}} \qquad [2]$$

Table 4. Range of dependent variables

Inlet liquid flow rate	14–21 kg/s
Liquid-to-steam flow rate ratio (ω)	3–14
Discharge liquid pressure	2.8–9.8 MPa
Discharge liquid temperature	61.5–193.9°C
Primary overflow pressure	90–478 kPa
Secondary overflow pressure	293–2541 kPa
Secondary overflow flow rate	7.2–17.6 kg/s

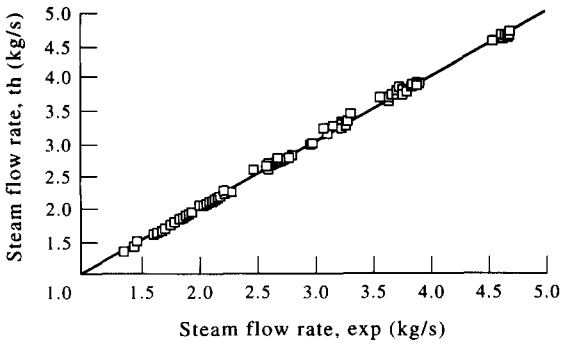

Figure 6. Steam nozzle: steam flow rate.

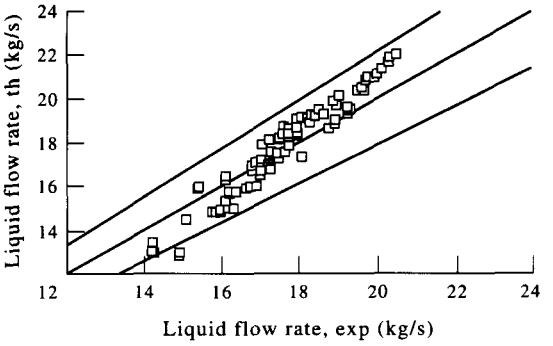

Figure 7. Liquid nozzle: calculated flow rate.

where Γ_G is the steam flow rate entering the injector, ρ_{G_a} is the steam density at steam nozzle exit and U_{G_a} is the steam velocity at the same position, derived from the steam enthalpies at the steam nozzle inlet and steam nozzle outlet sections:

$$u_{G_a} = \sqrt{2(h_{G_o} - h_{G_a})} \qquad [3]$$

It has been found that the corresponding calculated diameter (about 68 mm, approximately constant) is higher than the real steam nozzle outlet diameter (60 mm); on the other hand this value is always less than the total inlet mixing section diameter (72.4 mm). Indeed, steam flow leaving the steam nozzle tends to continue expansion, spreading along the mixing section.

Liquid nozzle performance

In order to calculate the liquid flow rate entering the mixing section through the liquid nozzle, the following equation can be used:

$$\Gamma_{L_a} = \rho_{L_a} A_{L_a} u_{L_a} \qquad [4]$$

where A_{L_a} is the liquid nozzle area, ρ_{L_a} is the density of the liquid entering the mixing section and u_{L_a} can be derived from the difference between the imposed inlet liquid pressure (P_{L_o}) and the liquid pressure at the steam nozzle outlet (P_{L_a}), taken to be equal to P_{G_a} ([1]):

$$u_{L_a} = \sqrt{\frac{2(P_{L_o} - P_{L_a})}{\rho_{L_a}}} \qquad [5]$$

In figure 7 experimental and calculated inlet liquid flow rates are shown and prediction is quite good.

Mixing section performance

Calculated temperatures at the OF2 sections (derived from an energy balance between the mixing section inlet area and OF2 area, assuming complete steam condensation) and measured liquid temperatures at the diffuser discharge section were found to be basically identical. This was confirmed by the measured temperature of the liquid leaving the SI through the OF2 opening (also, in this case, complete condensation was found). This indicates that in the mixing section complete steam condensation occurs. It can also be noticed that the pressure profile in the mixing section strictly follows the saturation profile, evaluated by heat balance on the liquid flow rate. Some theoretical models and correlations were proposed by Levy & Brown (1967), Brown & Levy (1972) and Miyazaki *et al.* (1973) to calculate the rate of heat transfer between the liquid–steam interface (of an annular two-phase flow) and the steam core. Nevertheless, none of these theories, developed for low pressure SIs, gives values of heat transfer coefficient able to match the experimental results; actually, steam condensation occurred with an efficiency much higher than that from theoretical prediction. This could be explained if a mixture atomization is assumed and a homogeneous

two-phase flow develops close to the mixing section inlet (so that the contact surface between steam and liquid is very large and direct heat transfer becomes very efficient).

Moreover, it was found that a compression shock always occurred, as registered by Fitzsimmons (1990), near to an overflow open section (regardless of whether it was secondary or primary).

Diffuser performance

The diffuser efficiency can be calculated as:

$$\eta_D = \frac{P_{o_e} - P_e}{KE} \quad [6]$$

where P_{o_e} and P_e are the measured pressures at diffuser outlet and inlet sections, respectively. The kinetic energy at the mixing section exit (KE) is:

$$KE = \rho_e \frac{u_e^2}{2} \quad [7]$$

where the liquid velocity at the mixing section exit (u_e) can be calculated as:

$$u_e = \frac{\Gamma_{L_a} + \Gamma_{G_a} - \Gamma_{OF2}}{A_e \rho_e} \quad [8]$$

where Γ_{L_a} and Γ_{G_a} are the liquid and steam flow rates entering the mixing section, equal to the liquid and steam flow rates entering the injector, Γ_{OF2} is the liquid flow rate leaving the injector through the secondary overflow, A_e is the area at mixing section exit and ρ_e is the liquid density at the mixing section exit.

An average diffuser efficiency has been taken for further calculations:

$$\eta_D = 0.65. \quad [9]$$

Discharge pressure performance

The injector discharge pressure for the entire test series is summarized in figure 8. In figure 9, the axial pressure profile at maximum inlet steam pressure is shown (the profile is similar at lower supply steam pressures). It should be remembered that the discharge pressure was fixed at an approximately constant value (10% higher than the inlet steam pressure), in order to meet the specifications. The tested one-stage SI developed sufficient discharge pressure except when the steam supply pressure was less than about 2.5 MPa.

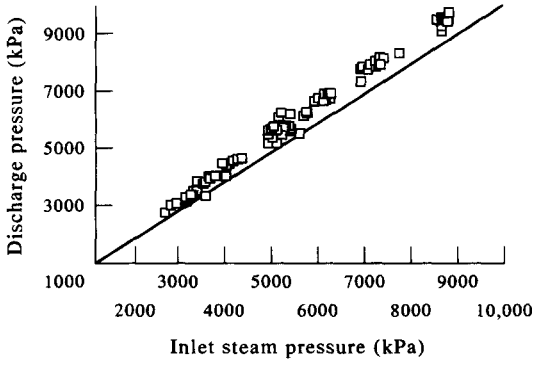

Figure 8. SI discharge pressure: experimental results.

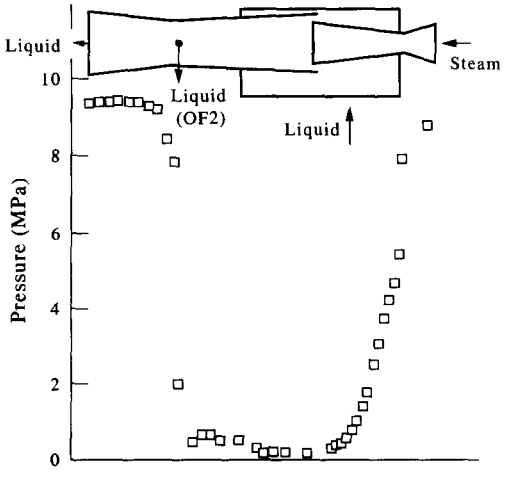

Figure 9. Experimental pressure profile along the test section.

The discharge pressure at the diffuser outlet (P_{o_e}) can be calculated as follows:

mixing section static outlet pressure (P_e) + diffuser pressure recovery (P_D)

On the other hand, taking into account that complete steam condensation occurs at the secondary overflow section, the mixing section static outlet pressure can be calculated as:

ideal pressure recovery at secondary overflow section (P_{OF2}) − "throat" pressure loss of condensated mixture at mixing section outlet (P_t).

In other words, it can be written as:

$$P_{o_e} = P_e + P_D = P_{OF2} - P_t + P_D \qquad [10]$$

The mixing section static pressure at the OF2 average section (i.e. the mixing cross section corresponding to the OF2 axis) can be calculated using an overall control volume analysis reported by Cattadori *et al.* (1992). The considered control volume is the mixing section, bounded by its inlet section *a* and the secondary overflow section (figure 10) where, as reported above, the steam is completed condensed. The following hypotheses can be assumed:

(a) steady-state conditions;
(b) no wall friction;

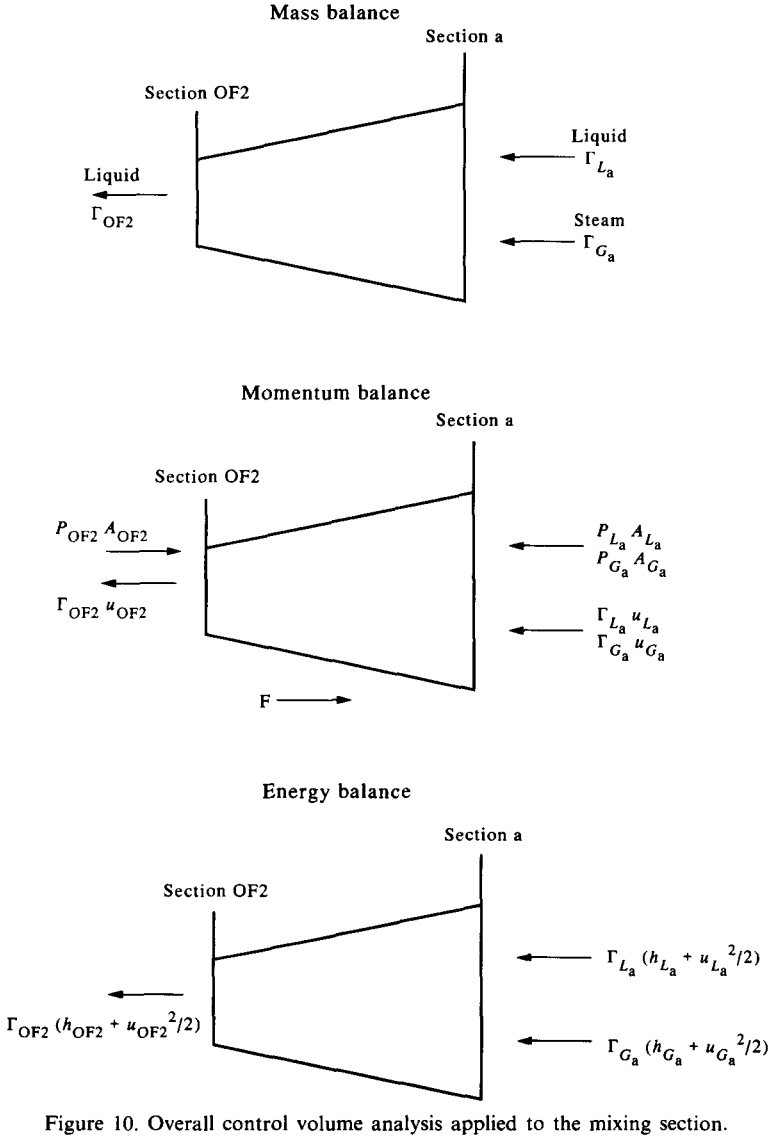

Figure 10. Overall control volume analysis applied to the mixing section.

(c) adiabatic walls;
(d) one-dimensional flow in section a and the OF2 average section: no radial gradient of temperature, pressure or velocity in each phase.

Mass, energy and momentum equations can be written between section a and OF2 (figure 10):

$$\Gamma_{L_a} + \Gamma_{G_a} = \Gamma_{OF2} \quad [11]$$

$$\Gamma_{L_a}\left(h_{L_a} + \frac{u_{L_a}^2}{2}\right) + \Gamma_{G_a}\left(h_{G_a} + \frac{u_{G_a}^2}{2}\right) = \Gamma_{OF2}\left(h_{OF2} + \frac{u_{OF2}^2}{2}\right) \quad [12]$$

$$P_{L_a}A_{L_a} + P_{G_a}A_{G_a} + \Gamma_{L_a}u_{L_a} + \Gamma_{G_a}u_{G_a} = P_{OF2}A_{OF2} + \Gamma_{OF2}u_{OF2} + F \quad [13]$$

Moreover, the continuity equation, written for section OF2, is:

$$\Gamma_{OF2} = \rho_{OF2}u_{OF2}A_{OF2} \quad [14]$$

The duct geometry (A_{L_a}, A_{G_a}, A_{OF2}) and the fluid inlet conditions being known, the four equations can be solved to obtain the outlet conditions (P_{OF2}, u_{OF2}, h_{OF2}, Γ_{OF2}) provided that an estimate is available for the axial component F of the wall forces. F, along the converging stretch of the mixing section, can be assumed to be proportional to the average saturation pressure at the inlet/OF2 sections (from experimental results, the pressure in the mixing section increases towards the throat following saturation temperature):

$$F = \alpha_1 \frac{P_{sat}(t_{L_a}) + P_{sat}(t_{OF2})}{2}(A_a - A_{OF2}) \quad [15]$$

where t_{OF2} can be derived by an energy balance between sections a and OF2 (assuming, as reported above, complete steam condensation at this section) and $A_a = A_{G_a} + A_{L_a}$ (A_{G_a} is the steam nozzle outlet area). The coefficient α_1 has been fitted with the collected experimental results to give:

$$\alpha_1 = 0.8 \quad [16]$$

Taking into account the above remarks the pressure recovery at the secondary overflow section can be calculated as:

$$P_{OF2} = \frac{P_{L_a}A_{L_a} + P_{G_a}u_{G_a} + \Gamma_{G_a}u_{G_a} + \Gamma_{L_a}u_{L_a} - F - (\Gamma_{L_a} + \Gamma_{G_a})u_{OF2}}{A_{OF2}} \quad [17]$$

The "throat" pressure loss, proportional to KE ([7]), represents the energy lost by the condensate mixture at the mixing section outlet. This can be calculated as:

$$P_t = \alpha_2 \mathrm{KE}. \quad [18]$$

The coefficient α_2 has been fitted with the collected data to give:

$$\alpha_2 = 2.0 \quad [19]$$

The diffuser pressure recovery can be derived from the calculated kinetic energy at the mixing section exit:

$$P_D = \eta_D \mathrm{KE} \quad [20]$$

where KE can be calculated from [8] and η_D is the experimental diffuser efficiency ($\eta_D = 0.65$).

The theoretical results (figure 11), calculated using [10], can predict the experimental results quite well.

Equation [10] can be used as a design equation for a rough SI calculation. Of course more sophisticated models should be used for a detailed design.

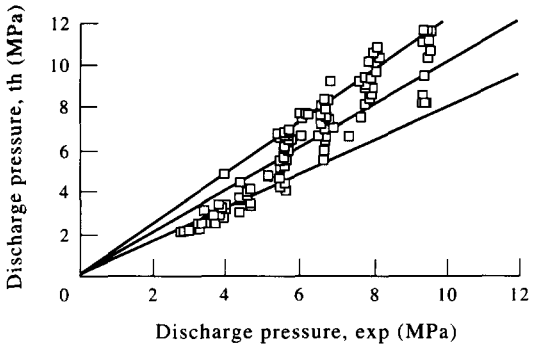

Figure 11. SI discharge pressure: calculated/experimental results.

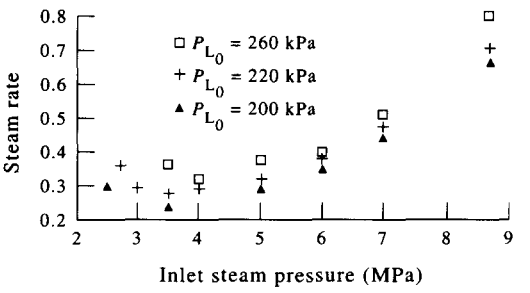

Figure 12. Steam rate (OF2 optimal setting). $T_L = 15°C$.

Steam consumption

Steam consumption is an important parameter in order to evaluate the performance of an injector. In particular specific steam consumption (steam rate, SR) can be defined as:

$$SR = \frac{\Gamma_{G_a}}{(\Gamma_{L_a} - \Gamma_{OF2})} \qquad [21]$$

In figure 12, SR values at different inlet water and steam pressures are shown in the case of the optimized OF2 setting (see appendix, test series I, optimized data). It can be seen that SR is quite low (< 1) and increases with inlet water and steam pressure.

It can be noticed that SR increases when inlet water temperature is increased (test series II). Indeed, the SI is most sensitive to the water supply temperature and inefficiencies increase with supply water temperature. In figure 13, SR values at different inlet water temperatures are shown.

In the case of a fixed OF2 opening (test series III) different valve positions were tested (figure 14). Even in this case the steam rate (SR) was quite low even if it was not possible to operate the SI in such a wide range as for previous tests with optimized OF2.

Anyway, it should be noticed that, at least at low liquid pressure and temperatures, SR is always less than 1 and steam consumption is reasonably low, thus SI can be efficiently applied to a BWR supplying the requested flow rate.

SI characteristic

Figure 15 shows a typical SI characteristic (from test series IV). The inlet steam pressure is 5 MPa and the inlet water pressure is 0.2 MPa. The inlet water temperature is 15°C. The

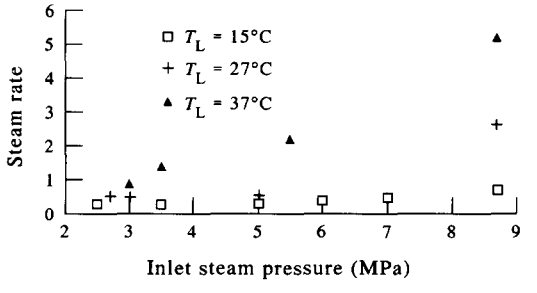

Figure 13. Steam rate: temperature effects ($P_{L_0} = 200$ kPa).

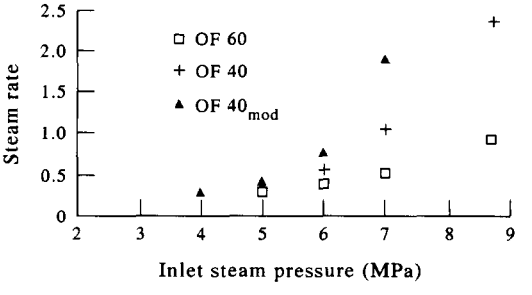

Figure 14. Steam rate: fixed OF2 opening ($P_{L_0} = 220$ kPa, $T_L = 15°C$). OF60: OF2 optimal setting corresponding to $P_{G_0} = 6$ MPa; OF40: OF2 optimal setting corresponding to $P_{G_0} = 4$ MPa; OF40$_{mod}$: OF2 slightly more open than OF40.

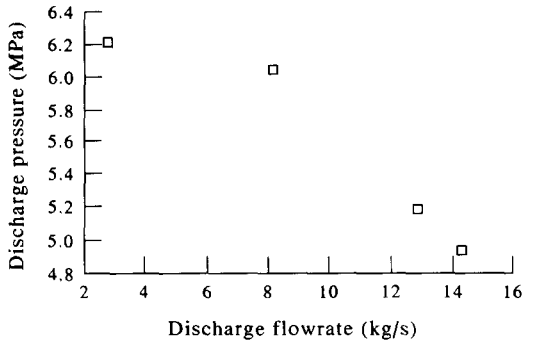

Figure 15. SI characteristic ($P_{L_o} = 200$ kPa, $T_L = 15°C$, $P_{G_o} = 5$ MPa).

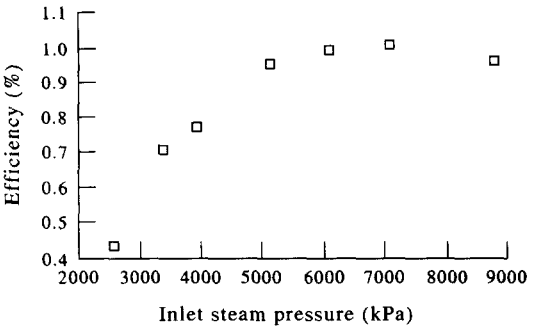

Figure 16. SI efficiency ($P_{L_o} = 200$ kPa, $T_L = 15°C$), OF2 optimal setting.

characteristic is similar to that for a centrifugal pump: the discharge pressure drops as the discharge flow rate becomes larger and larger.

It should be noticed that, in the case of a "low"-pressure injector, *without any overflow*, the injector performs as a positive displacement pump so that a constant flow rate is discharged against a range of back pressures, as noted by Grolmes (1968).

So an SI can be regarded as a positive displacement pump at "low" pressures (where high mixing section area contraction ratios are not required and overflow is not necessary) and a centrifugal pump at "high" pressures (where secondary overflow spillage is needed).

SI efficiency

Injector thermodynamic efficiency can be evaluated as:

$$\mathrm{EFF}(\%) = \frac{(P_{o_e} - P_{L_a})\dfrac{\Gamma_{o_e}}{\rho_{o_e}}}{\Gamma_{G_a}(h_{G_o} - h_{L_a})} \cdot 100 \qquad [22]$$

where Γ_{o_e} is the discharge flow rate and $\rho_{o_e}(=\rho_e)$ is the discharge liquid density.

In figures 16 and 17 the efficiencies calculated for optimized data ($T_L = 15°C$, $P_{L_o} = 200$ and 220 kPa) are shown; even if a direct comparison cannot be made, the observed behaviour is very similar to that of a mechanical centrifugal pump. In figure 18 the efficiencies calculated for different inlet liquid temperatures are shown for optimized data at $P_{L_o} = 200$ kPa (as the SI is very sensitive to the water supply temperature and inefficiencies increase with supply liquid temperature, the SI efficiency falls when the inlet liquid temperature is increased).

Flow rate spillage

The tested SI spills some of the water being pumped. In figure 19 spillage at a constant inlet liquid pressure (200 kPa) and different temperatures is shown; inlet steam pressure being constant, spillage

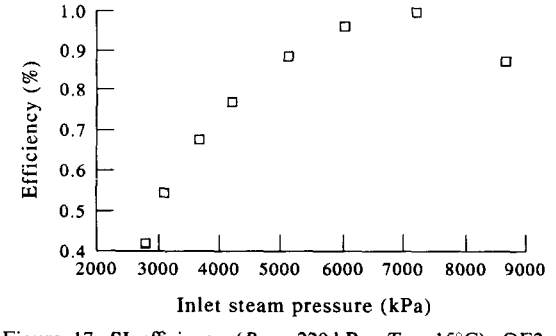

Figure 17. SI efficiency ($P_{L_o} = 220$ kPa, $T_L = 15°C$), OF2 optimal setting.

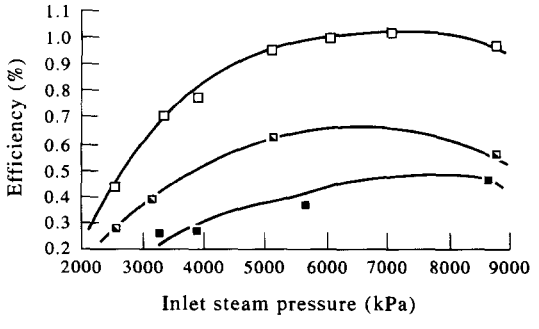

Figure 18. SI efficiency: temperature effects ($P_{L_o} = 200$ kPa).

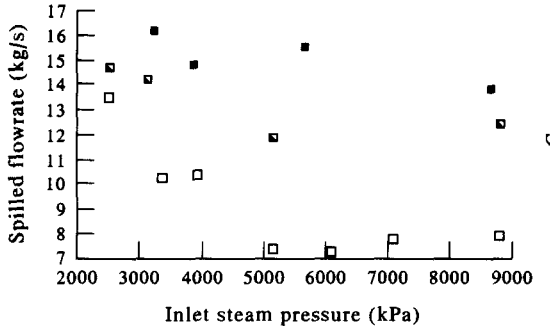

Figure 19. OF2 spillage: temperature effects (P_{L_o} = 200 kPa).

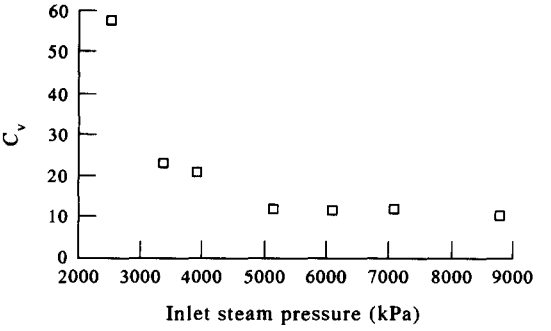

Figure 20. C_v trend (P_{L_o} = 200 kPa, T_L = 15°C).

increases with temperature. Indeed, at a fixed inlet steam pressure, efficiency drops with inlet liquid temperature and spilling increases.

In order to obtain useful data for the injector startup/flow rate control system design, the secondary overflow valve setting has been characterized using the flow rate coefficient C_v calculated as reported by Baumann (1963).

(a) Sub-critical conditions:

$$C_v = 0.037Q\sqrt{\frac{\rho_L}{\Delta P}} \qquad [23]$$

Q = volumetric discharged liquid flow rate through the secondary overflow (m^3/h)
ρ_L = discharged liquid density
$\Delta P = P_{OF2} - P_{back}$ (bar)

with P_{OF2} = pressure at the secondary overflow section and P_{back} = back pressure of the secondary overflow discharge valve (2 bar abs., constant value).

(b) Critical conditions:

$$C_v = \frac{0.037Q}{C_f}\sqrt{\frac{\rho_L}{\Delta P_s}} \qquad [24]$$

where:

$$\Delta P_s = P_{OF2} - \left(0.96 - 0.28\sqrt{\frac{P_{OF2}}{P_c}}\right)P_{sat}(t_{OF2}) \qquad [25]$$

C_f is an adimensional coefficient ("critical flow rate coefficient"), slightly dependent on valve type; $C_f = 0.9$ has been assumed; and P_c = critical pressure (221.2 bar).

The flow rate coefficient C_v versus the inlet steam pressure trend is shown in figure 20 at constant inlet liquid pressure (200 kPa) and temperature (15°C); C_v is always decreasing when P_{L_o} = 200 kPa.

Startup

In test series V, several tests were conducted modifying steps (a) and (d) in the startup sequence; in particular, before starting the tests, the back pressure and the secondary overflow valves were partially closed. Also the primary overflow valve was completely closed. Afterwards, the water and steam supply valves were opened and tests were performed at different inlet steam pressures and supply water pressures (the supply water temperature was always kept constant at 15°C). The SI could not always be started; results indicate that successful startup strongly depends on the inlet liquid pressure. In particular, with a partially closed back pressure valve (to give a discharge pressure 10% higher than the steam pressure) and "optimal" secondary overflow setting, startup was impossible (using the above described sequence) when steam pressure was lower than 5 MPa and P_{L_o} = 260 kPa. On the other hand, at P_{L_o} = 200 kPa, startup was easily obtained down to

$P_{G_0} = 3.5$ MPa. However, it should be noticed that these tests, at steady state conditions, can roughly simulate the real operating dynamic conditions where the back pressure valve is replaced by a check valve; in this last case startup may probably be easier.

Constant liquid-to-steam flow rate ratio tests

Even if the simplest steam injector configuration implies a constant inlet liquid pressures, several tests were conducted at an approximately constant liquid-to-steam flow rate ratio. In this case, the SI operating range was extended downwards; in particular, the injector could operate with an inlet steam pressure ranging from 1 to 8.7 MPa and the discharge pressure was up to 30% higher than the steam pressure. It is noteworthy that the primary and secondary overflow valves could both be completely closed during operation at a very "low" inlet steam pressure (< 2 MPa); in any other conditions some of the water being pumped was spilled from the secondary overflow (even if spillage was less than in previous tests where the inlet liquid pressure was kept constant).

4. SYSTEM AUTOMATION

An automatic double overflow flow rate control/startup system has been envisaged according to the scheme in figure 21, where two valves (1 and 2), connected to the OF1 and OF2 discharge lines, are shown. The OF1 line is provided for startup when the injector is full of water. Steam entering the injector would initially purge standing water in the mixing section and a steam–water mixture would flow through the OF1 discharge line to the suppression pool for several seconds until a sufficient suction flow rate has been established to enable full condensation of the steam in the mixing section and sufficient pressure is obtained to direct the flow to the reactor vessel. When a steady state flow has been established, the relief valve in the OF1 line will close due to the drop in static pressure inside the mixing section, resulting from the acceleration of flow in the mixing section itself.

As regards the secondary overflow, a valve controlled by steam pressure could be inserted on the OF2 line; in fact, optimal discharge flow through the OF2 line depends on the inlet steam pressure. This valve will tend to open at low inlet steam pressure, allowing a suitable liquid flow rate discharge; on the contrary, the OF2 valve would be almost closed at a high inlet steam pressure.

An additional possibility would be to modulate the inlet liquid flow rate by means of a valve controlled by the inlet steam pressure; in this case, at a constant discharged liquid flow rate, water consumption would be reduced and the operating range would be extended down to very low steam pressures.

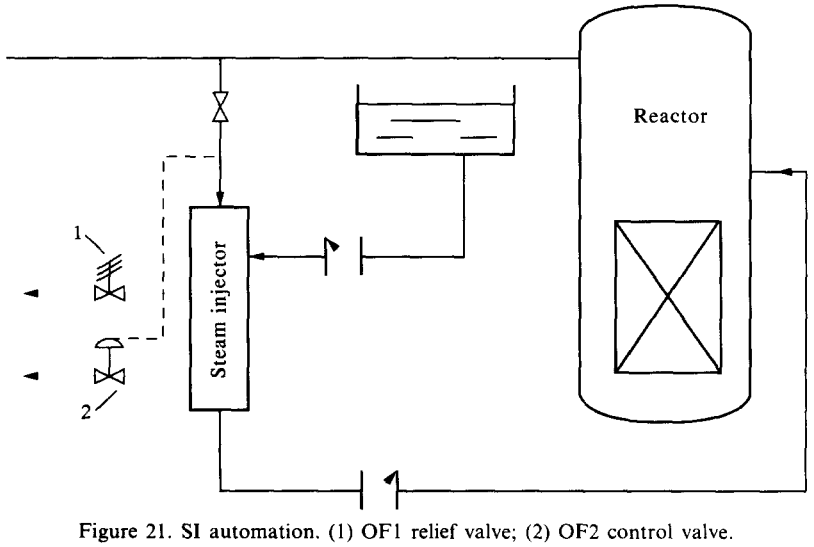

Figure 21. SI automation. (1) OF1 relief valve; (2) OF2 control valve.

5. CONCLUSIONS

The test results showed that the CISE one-stage high pressure SI can fully satisfy BWR safety injection requirements; in particular, the tested SI operates at a constant liquid pressure (about 0.2 MPa) with the steam pressure ranging from 2.5 to 8.7 MPa and supply water temperature ranging from 15 to 37°C, providing water to a discharge fixed pressure about 10% higher than the steam pressure. Moreover, it is noteworthy that the SI preheats the feedwater, which could be important for reducing the thermal stresses caused by relatively cold feedwater entering a hot reactor.

It should be noticed that:

- steam consumption is quite low and tends to increase with inlet liquid pressure and temperature and with steam pressure;
- the tested high pressure SI spills some of the water being pumped (at least at a constant supply water pressure). Spillage increases as the supply water temperature increases;
- the high pressure SI (due to secondary overflow spillage) can be regarded as a centrifugal pump.

REFERENCES

Baumann, H. D. 1963 The introduction of a critical flow factor for valve sizing. *ISA Trans.* **2,** 2.

Brown, G. A. & Levy, E. K. 1972 Liquid–vapour interactions in a constant area condensing ejector. *J. Basic Engng* **3,** 169–180.

Cattadori, G., Galbiati, L., Mazzocchi, L. & Vanini, P. 1992 Steam injector analysis and testing. *European Two-phase Flow Group Meeting*, The Royal Institute of Technology, Stockholm, Sweden.

Christensen, R. N., Aldemis, T. & Jayanti, S. 1987 An inherently safe BWR with a steam driven ECCS steam injector. *Energ. Nucl.* **2,** 30–37.

Fitzsimmons, G. W. 1990 Simplified boiling water reactor program. Steam injector system. Final Report, GE-NE.

Grolmes, M. A. 1968 Steam–water condensing-injector performance analysis with supersonic inlet vapor and convergent condensing section, ANL-7443.

Howard, R. W. 1984 Steam driven water injection. United States patent 4.440.719.

Levy, E. K. & Brown, G. 1967 Investigation of liquid–vapor interactions in a constant area condensing ejector. AFAPL-TR 67-105.

Miyazaki, K., Nakajima, I., Fujii, E. Y. & Suita, T. 1973 Condensing heat transfer in steam–water condensing-injector. *J. Nucl. Sci. Technol.* **10,** 411–418.

Narabayashi, T., Ishiyama, T., Miyano, H., Nei, H. & Shioiri, A. 1991 Feasibility and application on steam injector for next-generation reactor. *Ist JSME/ASME Joint International Conference on Nuclear Engineering*, Tokyo.

Narabayashi, T., Miyano, H., Nei, H., Ozaki, O., Mizumachi, W. & Shioiri, A. 1992 Feasibility study on steam injector driven jet pump for next-generation reactor. *69th JSME Spring Annual Meeting.*

Suurman, S. 1986 Steam-driven injectors act as emergency reactor feedwater supply. *Power* **3,** 95.

APPENDIX

Test Procedures and Test Program

The startup sequence in the tests was as follows:

(a) at the startup both overflow valves and the back pressure valve were opened;
(b) the water supply valve was opened first and most of the initial water flow was discharged through the overflow lines;
(c) when the steam supply valve was opened, condensation began in the mixing section;
(d) a strong vacuum developed in the mixing section and the primary overflow valve could be closed. At this point a performance optimization sequence was adopted;

(e) the OF2 valve was partially closed (avoiding any interference with the flow developed in the mixing chamber);
(f) the discharged back pressure could be increased by closing the back pressure valve until the discharge pressure was 10% higher than the inlet steam pressure. At this point data from the data acquisition system were recorded;
(g) the OF2 valve was closed step by step (each time setting the back pressure valve to always give a discharge pressure 10% more than the inlet steam pressure) until stalling was reached. After every back pressure valve setting, data were recorded.

Five test series were performed in the testing program.

Test series I

Using the above startup–optimization sequence, tests were performed at a constant inlet liquid pressure (three different water supply pressures were tested: 200, 220, 260 kPa) and temperature (15°C) for different inlet steam pressures. An optimal performance condition, corresponding to a 200 kPa inlet liquid pressure could be identified.

Test series II

At a constant inlet liquid pressure (200 kPa), the water temperature was increased up to 37°C, again using the described startup–optimization sequence.

Test series III

Several tests were conducted at constant inlet liquid pressure and temperature (220 kPa and 15°C) with a fixed setting of the secondary overflow; each time the discharge pressure was set at a value 10% higher than the inlet steam pressure while the inlet steam pressure was varied. Three different positions of the OF2 valve were tested, corresponding to those identified with the optimization sequence at the same inlet water pressure and temperature and P_{G_o} ranging from 4 to 6 MPa in test series I.

Test series IV

Tests were performed and an SI "characteristic" (similar to that of a centrifugal pump characteristic) was derived using the following procedure. The inlet liquid pressure and temperature were fixed, together with the inlet steam pressure. Then, at different back pressure valve positions, the OF2 valve was gradually closed until stalling.

Test series V

In order to investigate SI startup, several tests were conducted modifying steps (a) and (d) in the startup sequence; in particular, before starting the test the back pressure and the secondary overflow valves were partially closed and also the OF1 valve was completely closed. Afterwards, the water and steam supply valves were opened and tests were performed at different inlet liquid and steam pressures (at a constant inlet liquid temperature).